Results of a Search for Paraphotons with Intense X-ray Beams at SPring-8

9th Patras Workshop on Axions, WIMPs and WISPs

Toshiaki Inada
University of Tokyo

T. Namba, S. Asai, T. Kobayashi
University of Tokyo/ICEPP
Y. Tanaka, K. Tamasaku, K. Sawada, T. Ishikawa
SPring-8/RIKEN Harima institute

Based on Phys. Lett. B 722 (2013) 301

Paraphoton/Hidden Sector Photon

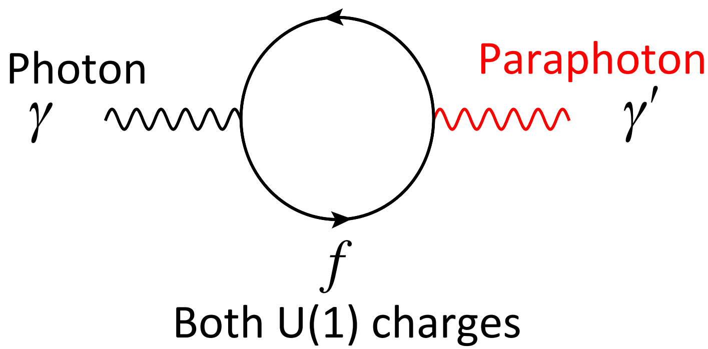

- Gauge bosons of hypothetical U(1) symmetry
  - Predicted by string-based extensions of Standard Model
- Tiny mixing with ordinary photons
  - Neutrino-like flavor oscillation

- Precise test of QED
- Abnormal heat transfer mechanism in stars
- One candidate of dark matter

Oscillation Probability for LSW Experiments

- Oscillation of the probability of $\gamma \rightarrow \gamma'$ and $\gamma' \rightarrow \gamma$

- Axion LSW by S. L. Adler et al (2008) ⇒ Paraphoton LSW

$$P_{\gamma\to\gamma'} = \left(\frac{\omega + \sqrt{\omega^2 - m_{\gamma'}^2}}{\sqrt{\omega^2 - m_{\gamma'}^2}} \chi \right)^2 \sin\left(\frac{L}{2}\left(\omega - \sqrt{\omega^2 - m_{\gamma'}^2} \right) \right)$$

- For $m_{\gamma'} \ll \omega$

Paraphoton mass

$$P_{\gamma\to\gamma'} = 4\chi^2 \sin^2\left(\frac{m_{\gamma'}^2}{4\omega} L \right)$$

Oscillation length (fixed by setup)

Photon energy

Mixing angle

- Probed mass scales to the photon energy
  - Sources with different energies are important for extending the LSW limits

Current Terrestrial Limits

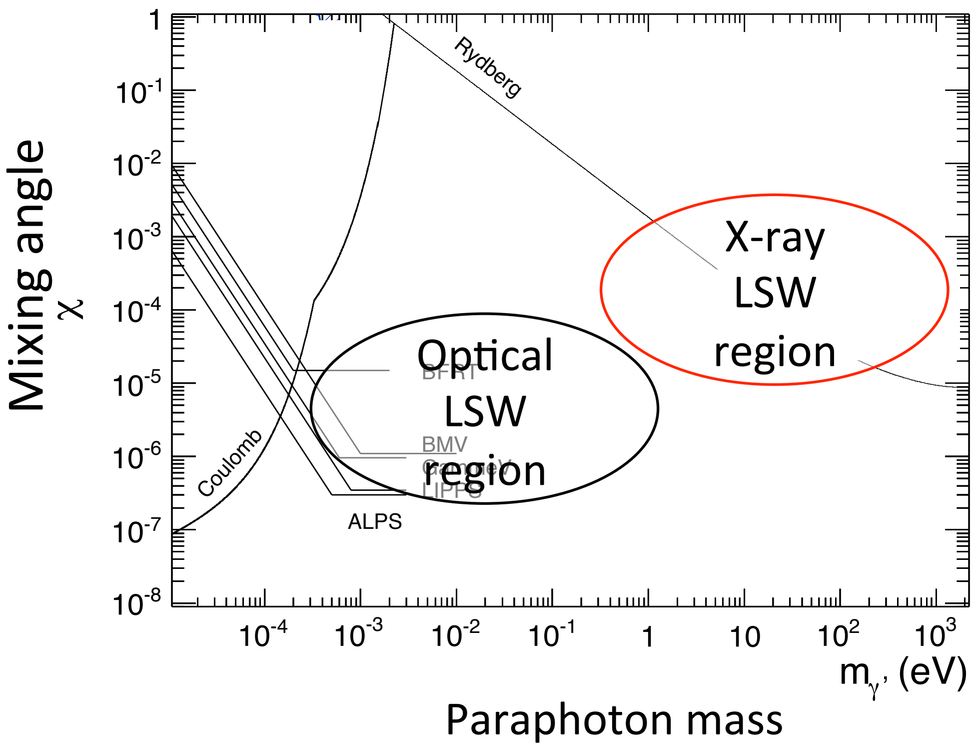

- Optical LSW range: meV – eV
- Below this: Microwave
- Above this: X-ray region

- Purely terrestrial- and intense X-ray source
- Synchrotron radiation facility

⇒ R. Battesti et al (2010) @ ESRF for axion-LSW

- Extends LSW limits to higher masses

X-ray Intensity Frontier SPring-8 and our beamline BL19LXU

- SPring-8 (Super Photon ring at 8 GeV)
- 62 beamlines around 1.42 km electron ring
- X-rays from soft (∼1 keV) to hard (∼ 100 keV)

- BL19LXU (BeamLine 19 Long X-ray Undulator)
- 30-m-long in-vacuum undulaot

⟹ Most intense X-rays available today as a continuous beam

BL19LXU	Value (after monochromator)
Output energy	7.2–51 keV
Beam intensity	10^{13}–10^{14} photon/s @7.2–30 keV
Line width	∼eV (FWHM)
Beam size	∼400 μm (FWHM)
Pulse width/interval	40 ps/24 ns (∼CW)

Beam Energies and Fluxes

- 9 energies are used
- Fluxes of higher harmonics are relatively weaker

$\Longrightarrow$ We used 1st/3rd harmonics

harmonics	used energy (keV)	flux (photon/s)
$n = 1$	7.27, 8.00, 9.00, 15.00, 16.00, 17.00	10^{14}
$n = 3$	21.83, 23.00, 26.00	10^{13}

- Measured with a Si PIN photodiode
- Accuracy better than (avg.) 2%

Overview of Experimental Setup and Definition of the Oscillation Regions

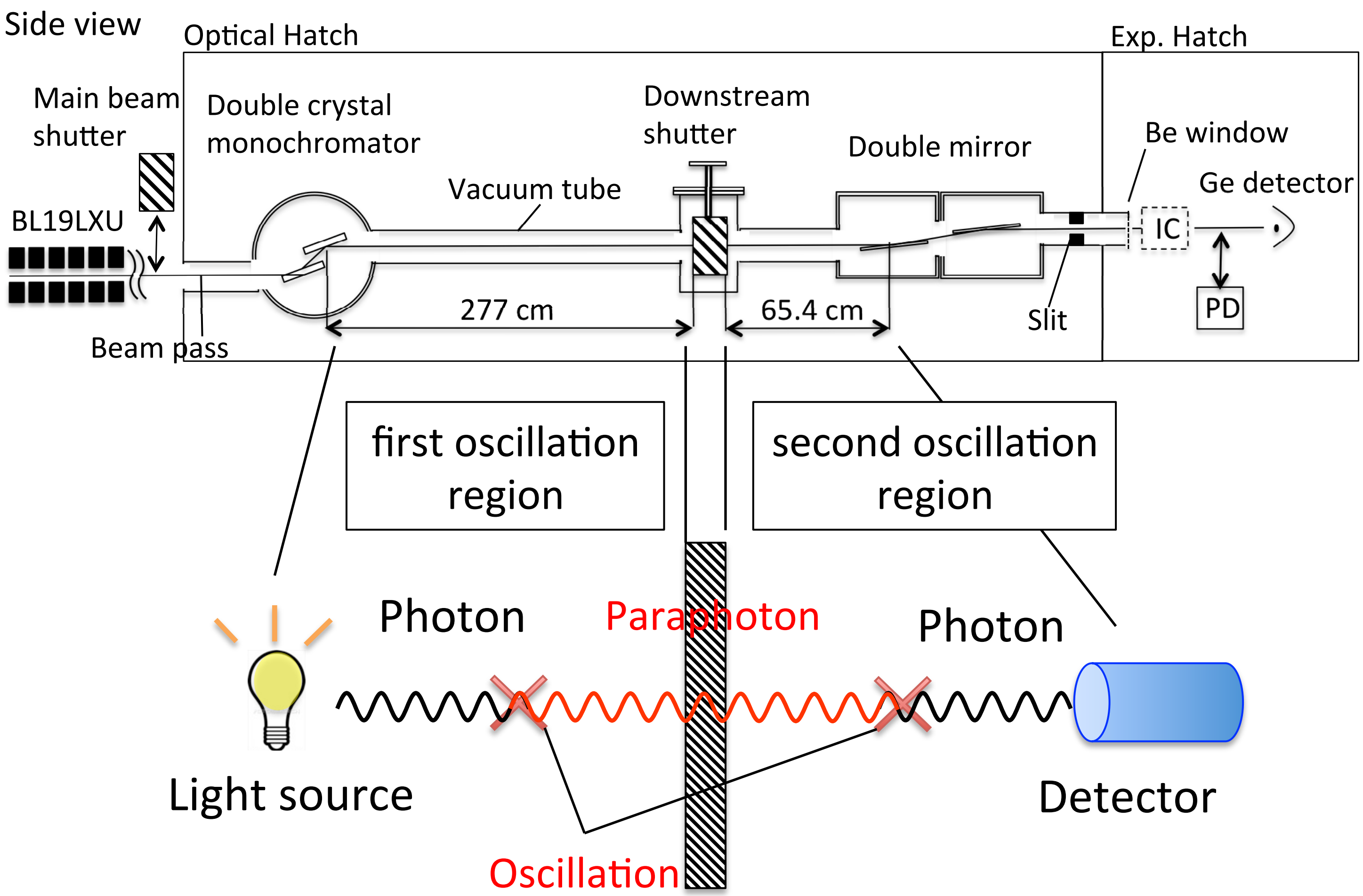

Overview of Experimental Setup and Beamline Components

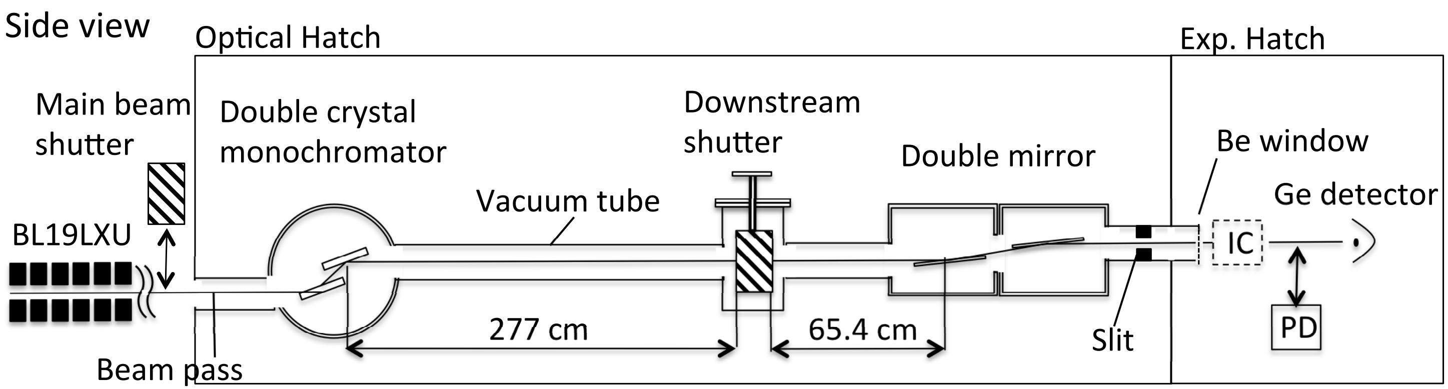

- Beams from the undulator has a continuous spectrum

⟹Monochromated to $\Delta\omega/\omega \sim 10^{-4}$ with a Bragg condition

- Blocked by a 94-mm-thick lead shutter
- Only LSW photons are selected by a pair of total reflection mirrors
- Detected with a germanium detector in a experimental hatch

Overview of Experimental Setup and Beamline Components

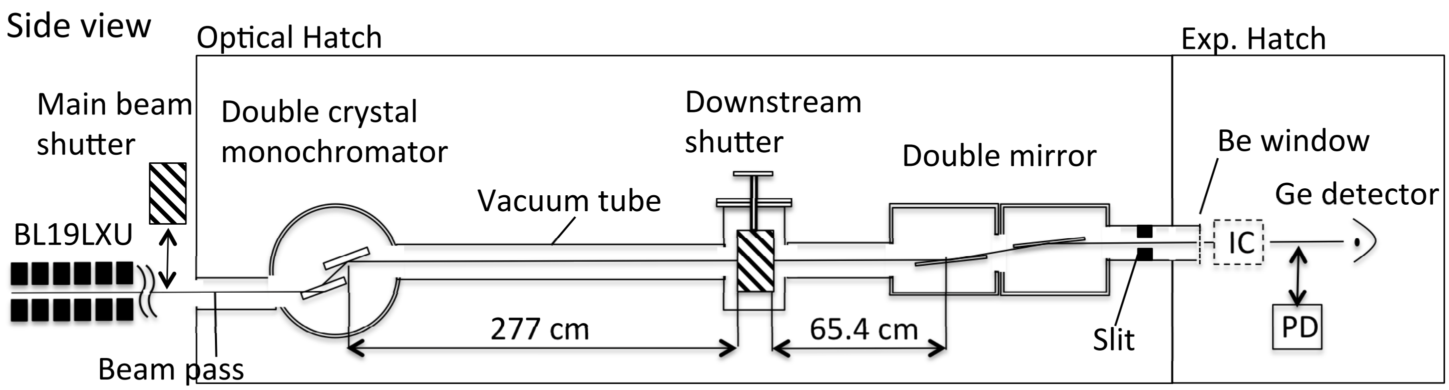

- Upstream -

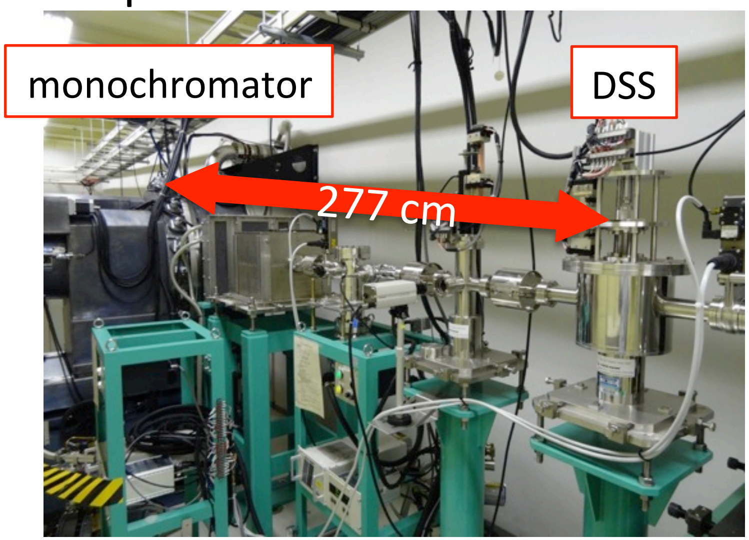

- Downstream -

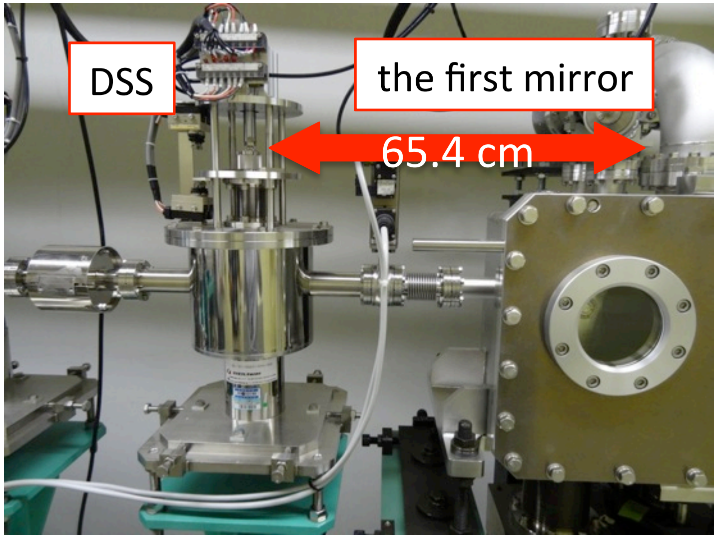

Detection System - Setup -

- Inside the experimental hatch -

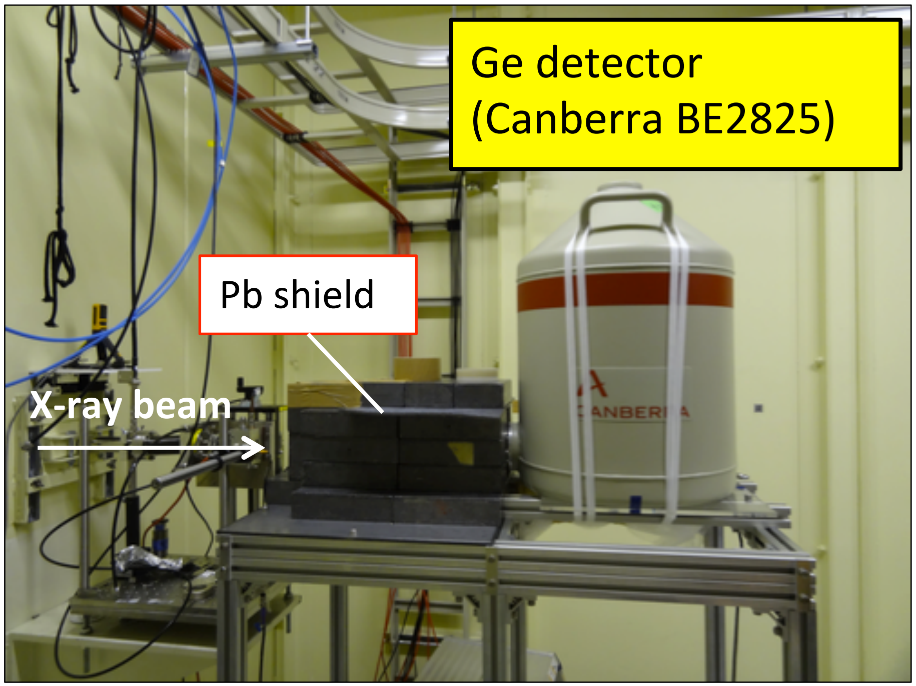

- ϕ60 germanium crystal
- Shielded by 5 cm-thick leads
- Beams are injected through a ϕ30 collimator
- Energy spectrum is recorded by a peak-holed ADC for energy cuts

Component	Value
Ge crystal	diameter 60 mm thickness 25 mm
Detector window (CFRP plastic)	thickness 0.6 mm
Pb shield	thickness 50 mm
Beam collimator	diameter 30 mm

Energy Resolution of Ge Detector and Definition of Signal Region

- ^{57}Co spectrum -

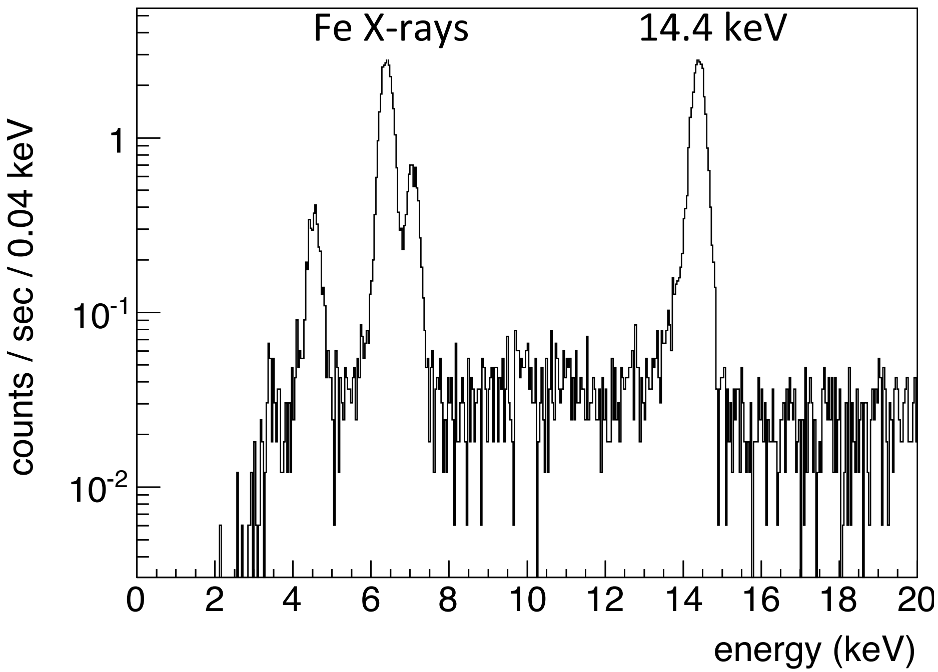

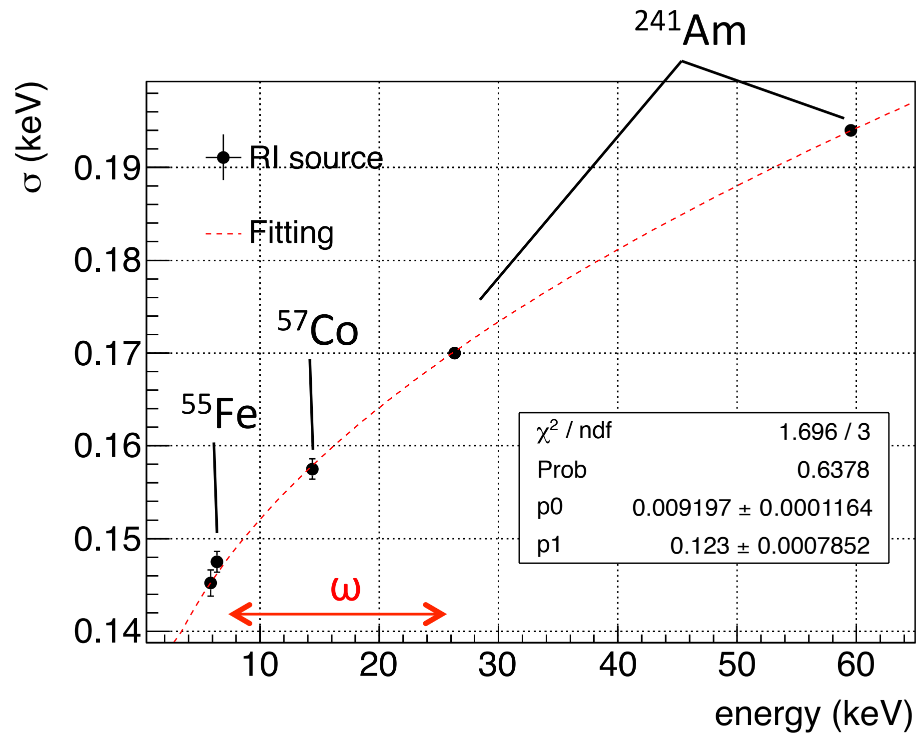

- Measured with RI sources
  - <u>157 eV (σ) @ 14.4 keV from ^{57}Co</u>
- Interpolated by the function of $\sigma = p_0\sqrt{E} + p_1$ (keV)
- <u>Defined beam energy ±2σ as a signal region</u>

Detection Efficiency

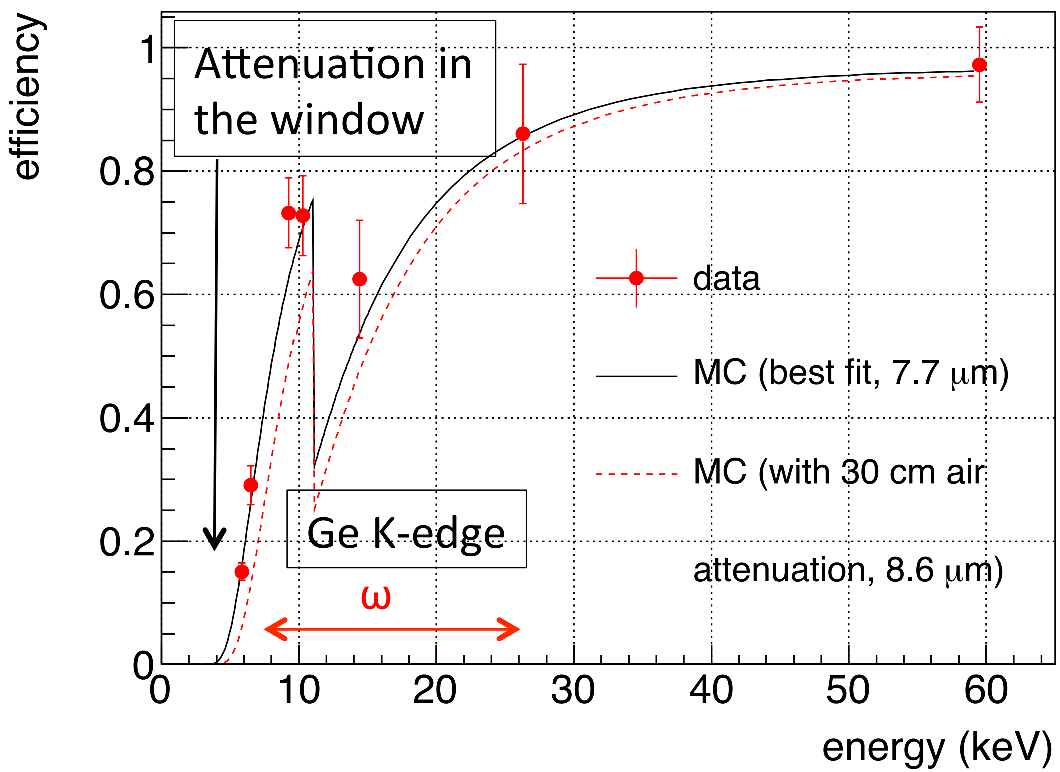

- Also measured by RI sources
- Thickness of surface dead layer is crucial for inefficiency around Ge K-edge

⇒GEANT4 simulation with the thickness as a free parameter

- Conservative curve of 1σ deviation including air attenuation (dashed red) is used in the analysis

Typical efficiencies: 23% @ 7 keV and 83% @ 26 keV

Setup of Main Measurements with Beam ON and OFF

- Beam ON
- Change beam energy for 9 times
- Livetime on each measurements: 5-9 hours

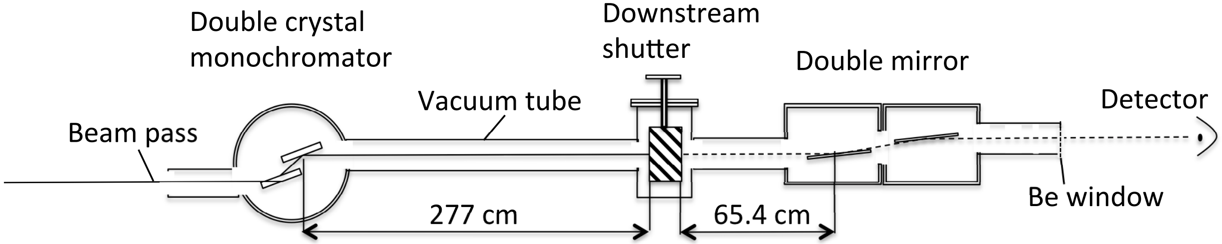

- Beam OFF
- Completely the same setup except for closing the main beam shutter
- 45.5 hours of livetime

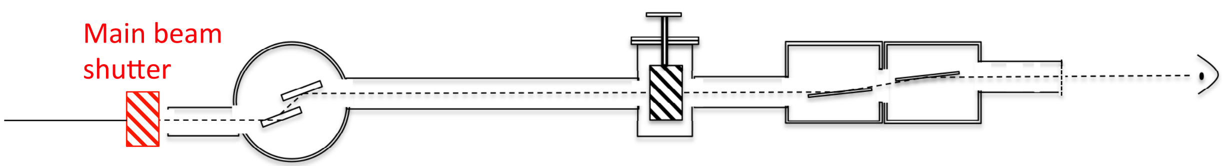

- Paraphoton signal
- Statistically significant difference of the detector count rates between ON and OFF

Background Spectrum

- Arrows show the signal regions of 9 measurements
- No overlaps => commonly used for subtraction

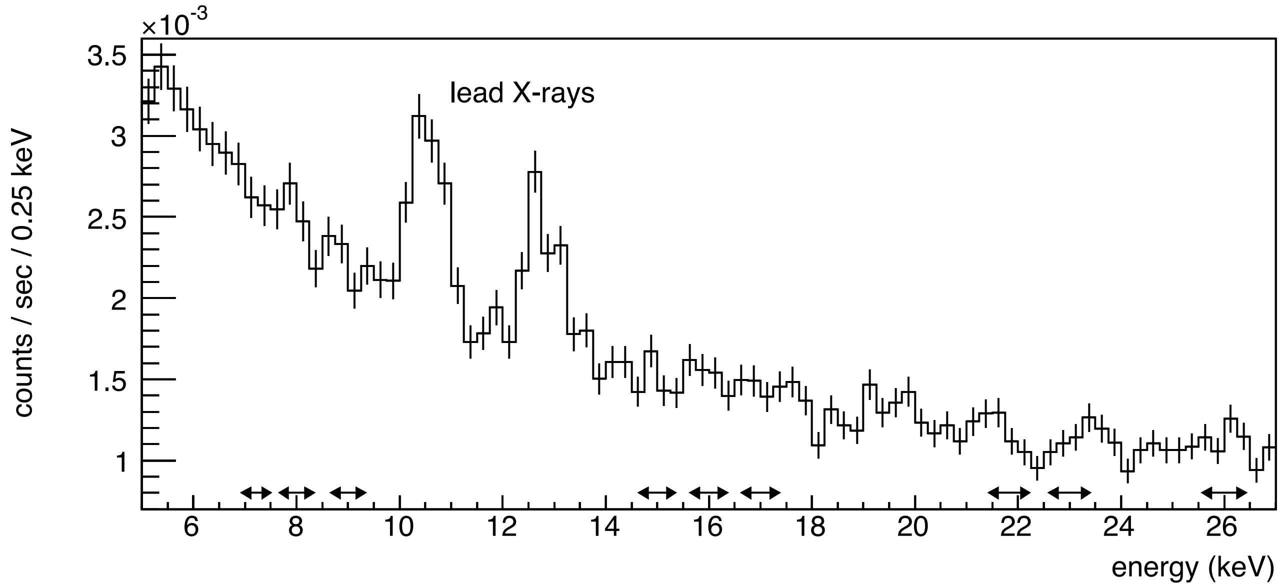

- 10.5 keV and 12.7 keV peaks: Lead X-rays from shields and a collimator
- Avoided for the choice of beam energy
- Except for this, normal continuous spectrum
- BG rate in each signal region is ∼ a few mHz

Background-Subtracted Spectrum

- One example of 9 keV measurement
- Bars are statistical errors (1 sigma) and signal region data with red points
- Paraphoton-like signal over +2 standard deviations was not detected!

  <u>(Also with the other energy measurements)</u>

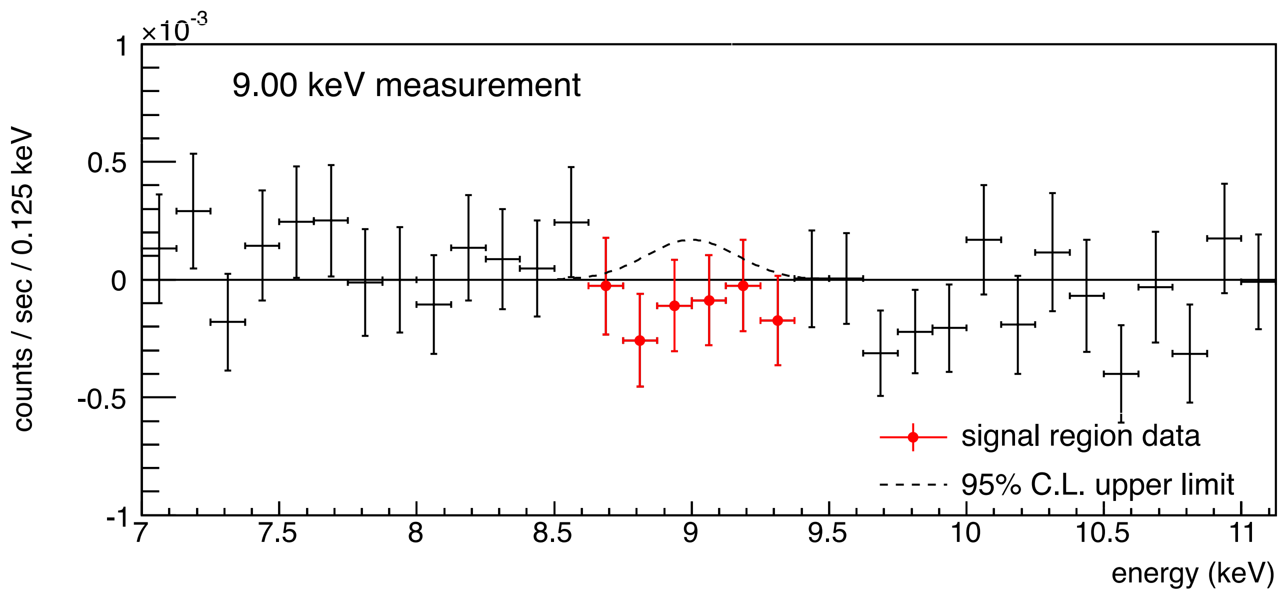

- Hereafter, focus on the discussion of constraining the mixing angle
- Dashed line: a signal upper limit（95% C.L.） calculated from total counts in the signal region

Background-Subtracted Spectrum
The Other Energy Measurements

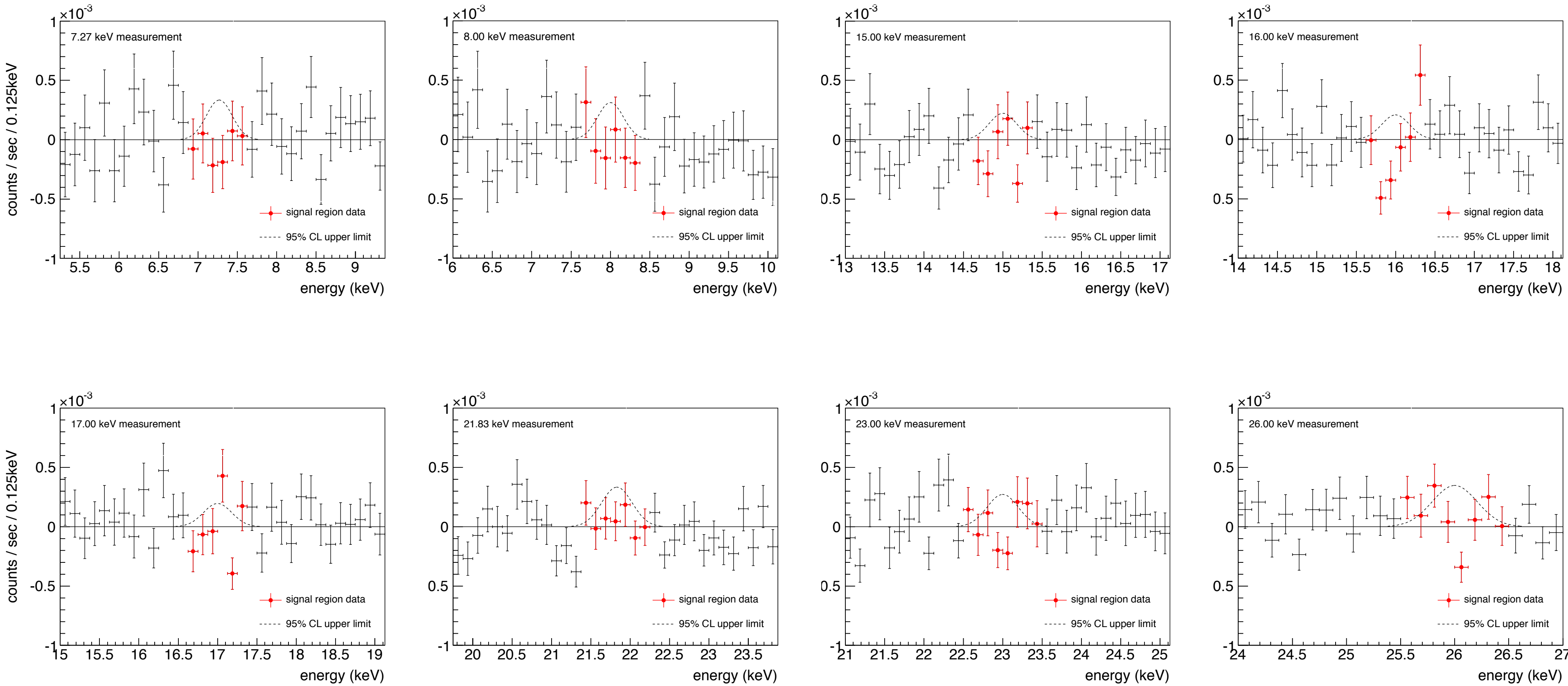

Significant excess was not observed

Calculation of Mixing Angle

- Vertical direction with y axis

$$\epsilon \boxed{I \int P_1(y)\ P_2(y)\ \rho(y)\ \mathrm{d}y} = \Delta N_{95\%\mathrm{C.L.}}$$

Detection efficiency

Photon flux (s^{-1})

LSW-photon flux (s^{-1})

Signal upper limit (s^{-1})

- ρ(y): Beam profile along the y direction
  - Normalize its area to a unit
- Neutrino-like conversion probability

$$P_i(y) = \left[2\chi \sin\left(\frac{m_{\gamma'}^2\ L_i'(y)}{4\omega}\right)\right]^2$$ (for low masses)

  - Depends on L, the oscillation region length!

Beam Size

- Space structure
  - Measured with a slit scan along horizontal/vertical direction with a 10 μm pitch
  - Vertical width ∼ 400 μm (FWHM)

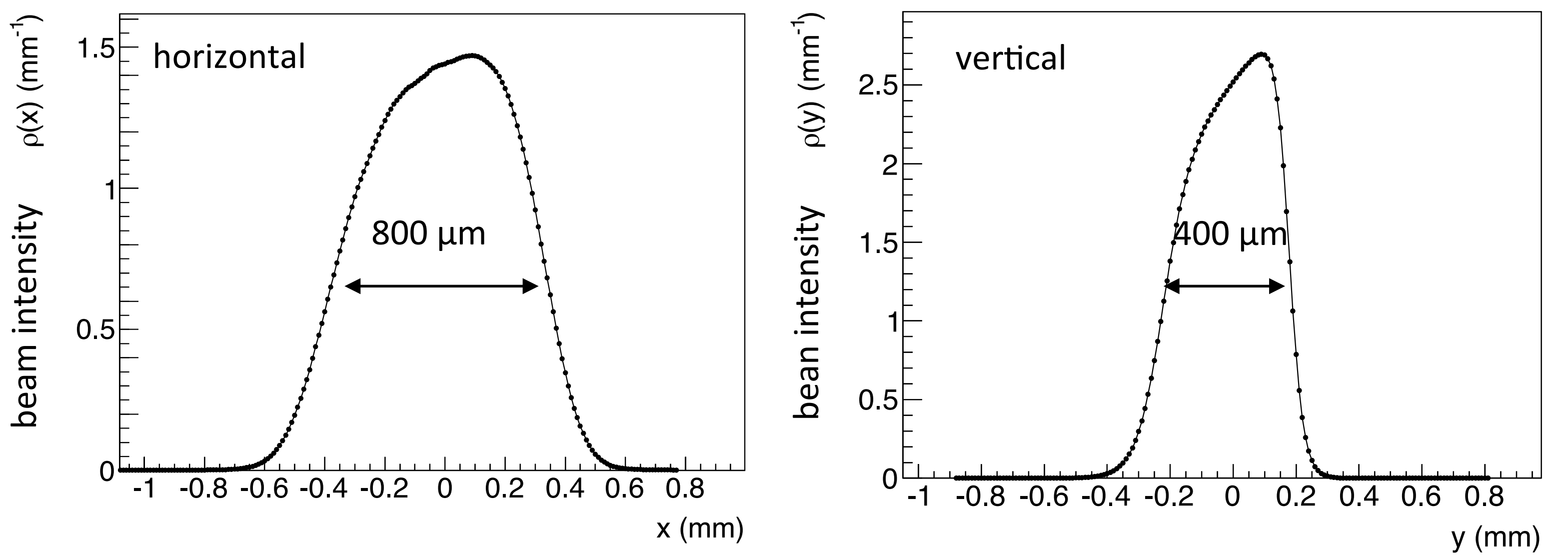

Tilting Edges and Beam Width Effect

- Both edges of oscillation region (i.e. monochromator and first mirror) have shallow angles along the beam axis
- Length of oscillation region changes with respect to the local y positions!

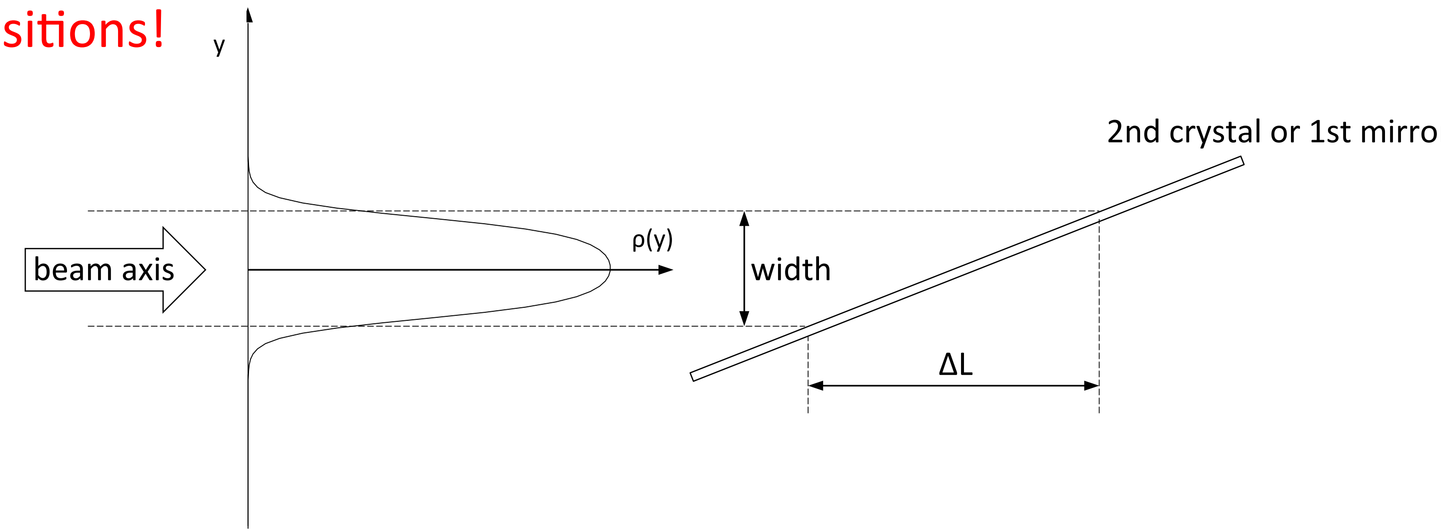

- ΔL variances from beam width (～400 μm)
- First oscillation region: a few mm <= Bragg angle ～100 mrad
- Second oscillation region: ～10 cm <= total reflection angle ～few mrad
- Integrate over each y contributions

Limits on the Mixing Angle

- 95% C.L exclusion limit (upper side is excluded)
- One example from a single 9.00 keV measurement

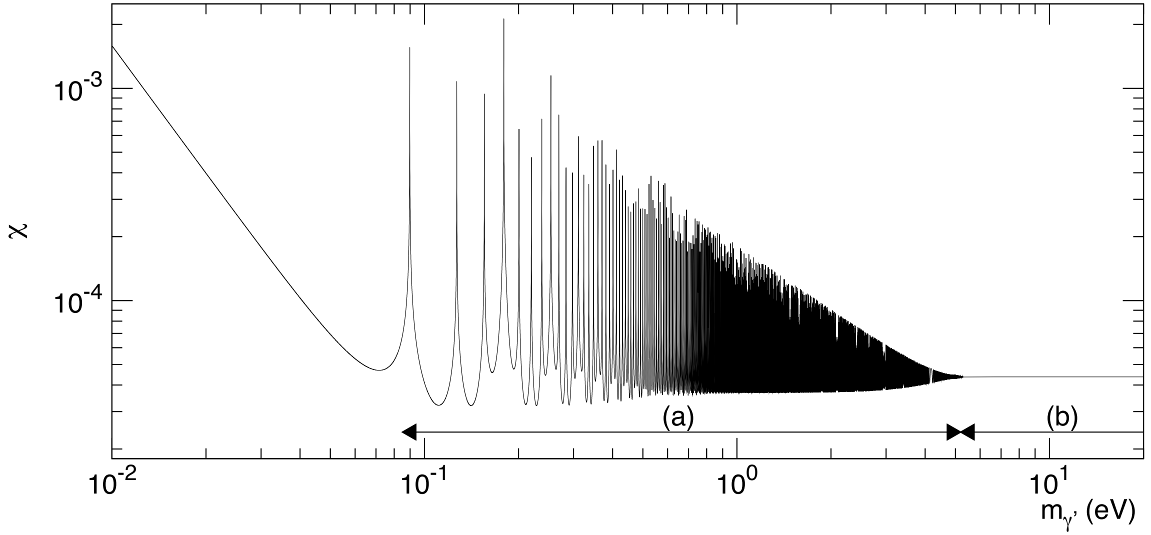

- Region (a): spiky structure from the sin functions of oscillation probabilities
- Region (b): smeared out due to the integration
- For heavy masses: oscillation length < ΔL variance

Combination of the Results

- Obtain a combined result by the same procedure using χ^4 distributions and multiplying each others
- Spiky structures of the region (a) are compensated with 9 measurements

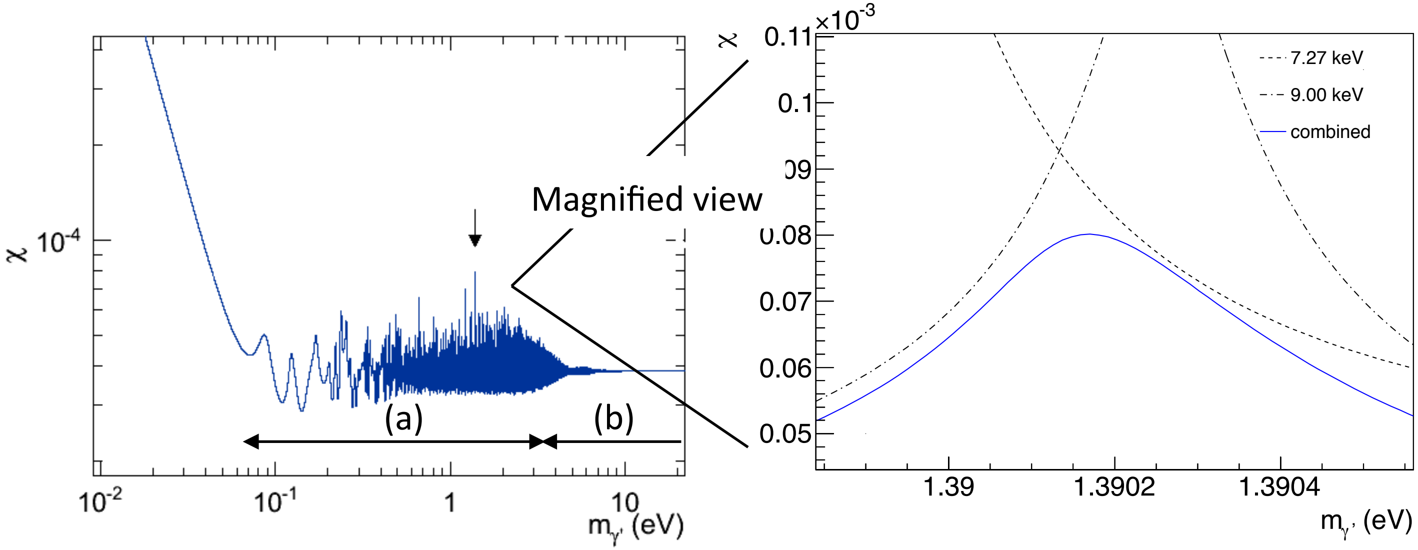

- The worst value appears at 1.39 eV:

$$\chi_{worst} = 8.01\times 10^{-5}$$

- Represents our result

Systematic Errors

- Uncertainties of the beam intensities and detection efficiencies
- Already taken into account by using 1σ decreased conservative values(*)
- The other uncertainties: energy scale and oscillation region length

Factor	Contribution to $\chi_{\rm worst}$
*Beam intensities	(avg.)± 0.40 %
*Detection efficiencies	(avg.) $^{+0.64}_{-0.83}$ %
Absolute energy scale ($\Delta\omega = -18$ eV)	$< \pm 0.01$ %
Oscillation lengths ($\mathrm{L}_1 = 277 \pm 2$ cm, $\mathrm{L}_2 = 65.4 \pm 0.5$ cm)	$^{+0.52}_{-0.15}$ %

- Appear in the phase of sin function
- Cause a shift of the whole limit line along the mass axis

  ⇒ Traced χ_{worst} by changing the two parameters and listed maximum deviations

- χ_{worst} + 0.52% represents our final result:

$$\chi < 8.06 \times 10^{-5} \quad \text{(95\% C.L.)}$$

Comparison of the Results

- Probed mass region up to 26 keV

- 4-order-heavier than optical LSW ～ev

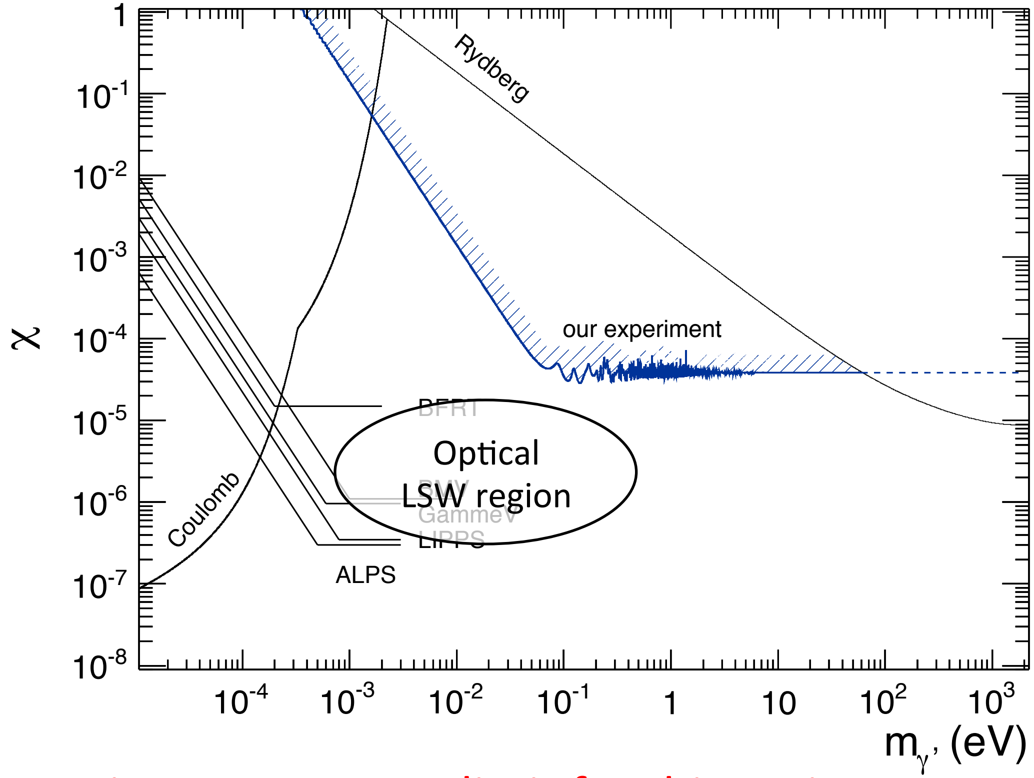

- Most stringent as a LSW limit for this region

Further Prospects 1/2
Paraphoton Search

- New X-ray source: Free Electron Laser, SACLA
  - In public use since last year, and reaches to the designed performance in next year
  - The same flux (s^{-1}) with SPring-8 and pulsed beam
    ⇒ Pulse width ～10 fs
- Time window of detector coincides with beam pulse
  - Zero background count

2-order-improvements of S/N
for one week measurement

Further Prospects 2/2
Axion-like Particle Search

- Introduce photon-ALP conversion magnets to the paraphoton setup

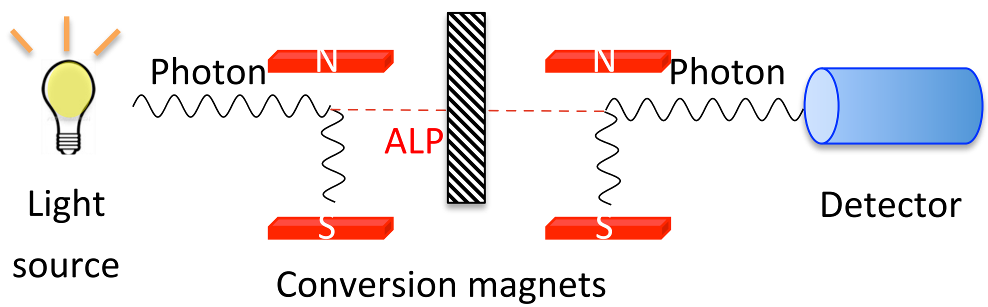

- Already maintains eight dipole magnets decommissioned from KEKB
  - 2 T × 2.1 m × 8

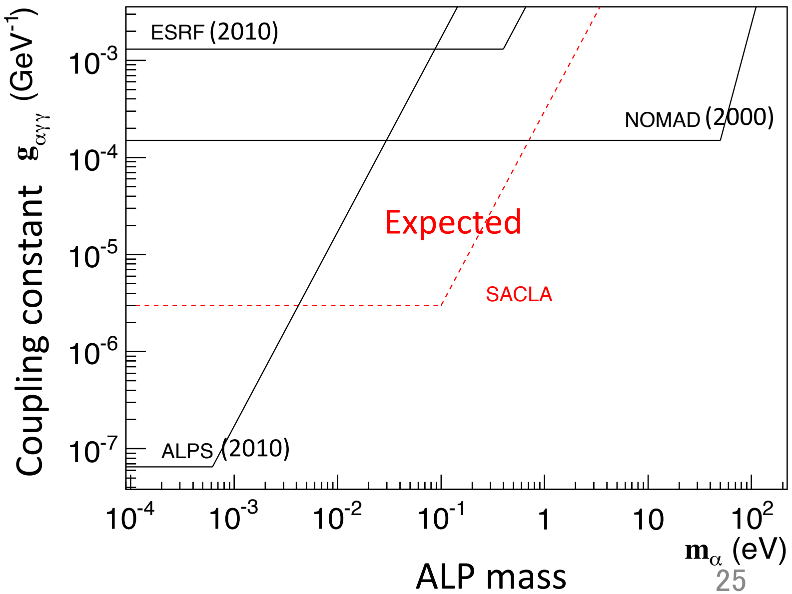

<u>Improvement by factor 40 from NOMAD (2000) is expected</u>

Summary

- Paraphoton search using intense X-ray beams was performed at SPring-8.
- LSW method was applied and wall-penetrating LSW photons were searched with Ge detector.
- From the absence of paraphoton signals, a new experimental constraint was obtained:

$$\boxed{\chi < 8.06 \times 10^{-5} \quad (0.04\ \text{eV} < m_{\gamma'} < 26\ \text{keV, 95\% C.L.})}$$

- Probed mass region is 4-order-heavier than optical LSW searches

Measurement of Intensities 1/2
Setup

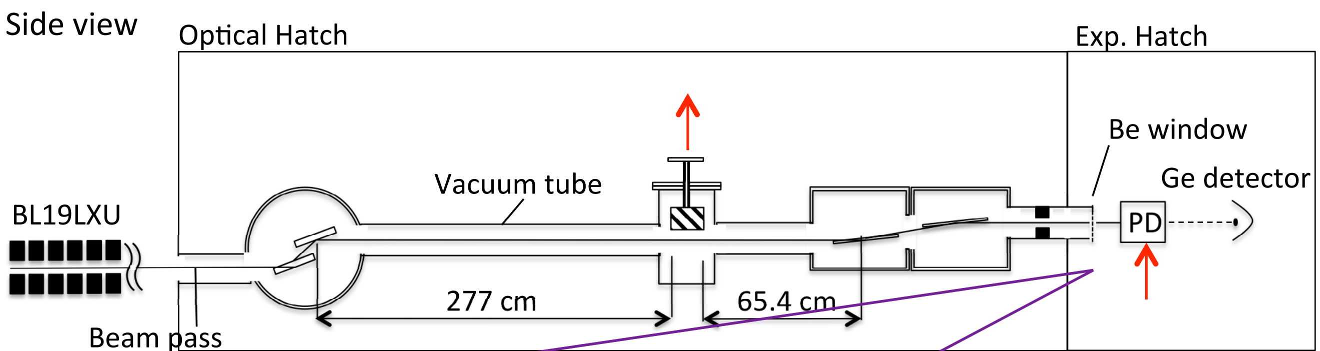

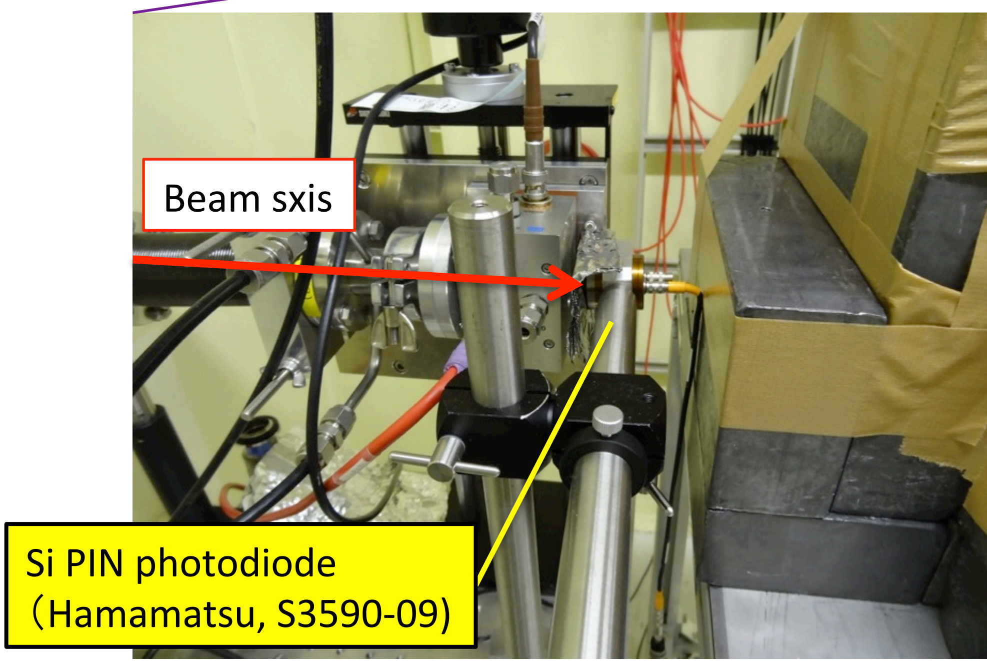

- Insertion PIN photodiode on the beam axis
- Protection of the detector with lead shields
- Shutter open and injection of the beam

<u>Measurements are performed every 3-4 hours</u>

Measurement of Intensities 2/2
Calculation of Fluxes from PIN currents

- e/h pairs created by energy deposit within a 300-μm-thick Si (W_{si}=3.66eV)
- Currents are read out with a picoammeter

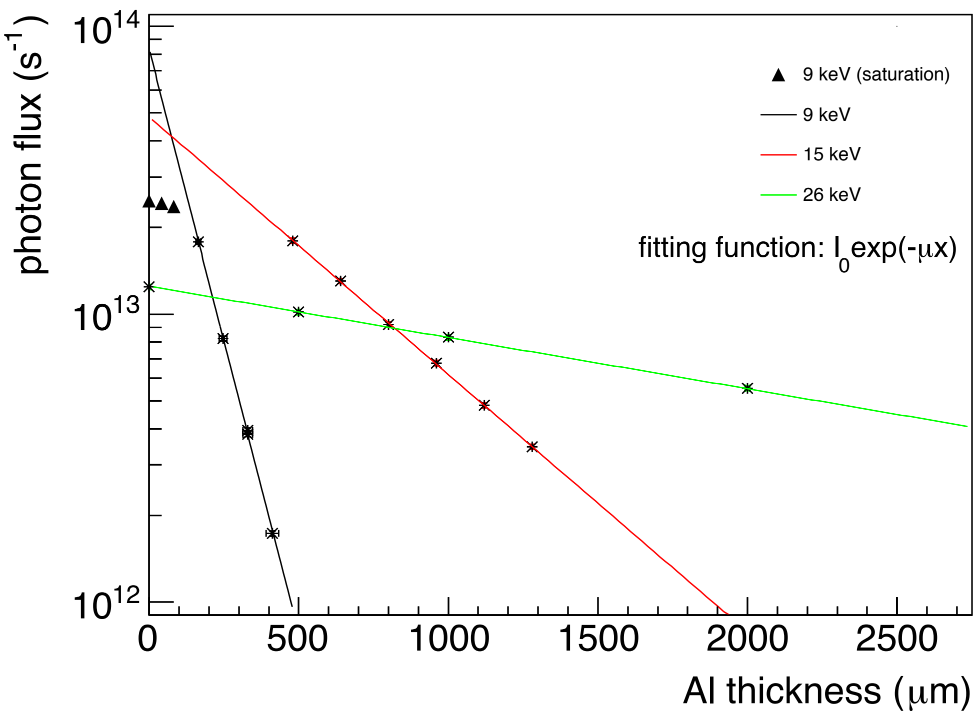

- Direct beam ⇒ Current saturation
- Attenuation with Al sheets
- End points are extrapolated
- Attenuation coefficients are calculated with GEANT4 and fixed on fittings

Accuracy of measurements is less than (avg.) 2%

Calculation of Signal Upper Limit

- Gaussian distributions are assumed from the center value and standard deviation of ΔN (subtracted counts in the signal region)
- 95% position of the total area, defined only for physical (i.e. positive) region), is taken as 95% C.L.

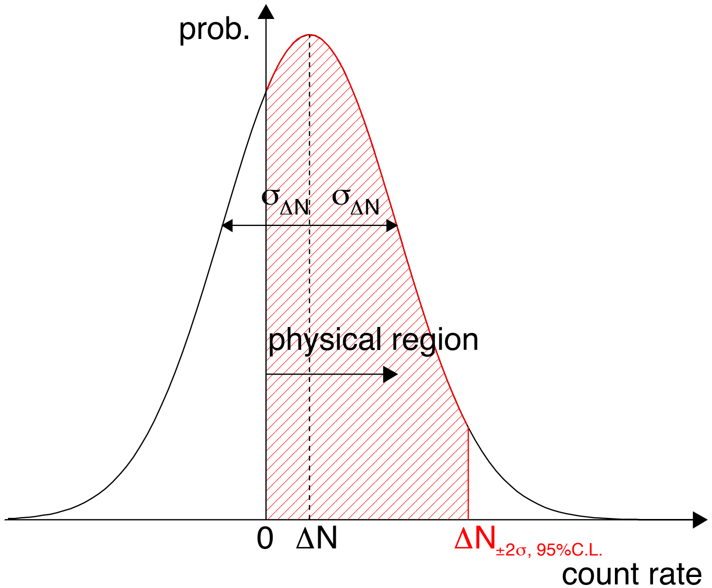

- Signal content rate in (ω±2σ) is 0.9545, and upper limit is obtained from

$$\Delta N_{95\%C.L.} = \frac{\Delta N_{\pm 2\sigma, 95\%C.L.}}{0.9545}$$

Cross Section of the Magnet

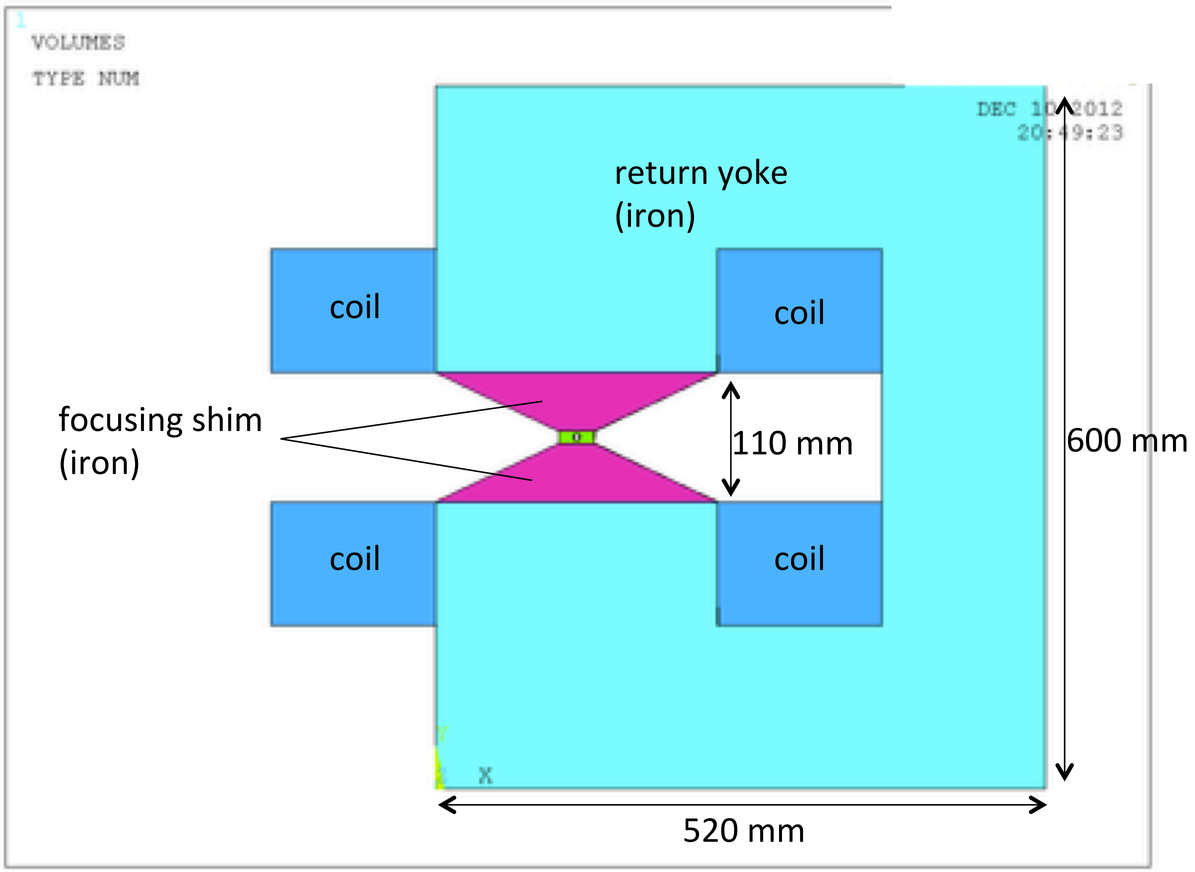

Dataset

beam energy ω (keV)	livetime (h)	detector resolution σ (keV)	beam intensity I (10^{13} s^{-1})	detector efficiency ϵ (%)	$N_{\rm beam} \pm$ (stat.) in $(\omega \pm 2\sigma)$ (10^{-3} s^{-1})	$N_{\rm BG} \pm$ (stat.) in $(\omega \pm 2\sigma)$ (10^{-3} s^{-1})	$\Delta N \pm$ (stat.) in $(\omega \pm 2\sigma)$ (10^{-4} s^{-1})	$\Delta N_{95\%\rm C.L.}$ (10^{-4} s^{-1})
7.27	7.0	0.16	7.6	23	7.0 ± 0.5	7.1 ± 0.2	-0.9 ± 5.7	11.0
8.00	5.4	0.16	8.9	33	6.5 ± 0.6	6.9 ± 0.2	-3.8 ± 6.1	10.3
9.00	8.8	0.17	8.3	46	5.3 ± 0.4	6.0 ± 0.2	-7.6 ± 4.5	5.5
15.00	5.2	0.18	4.6	51	4.2 ± 0.5	4.5 ± 0.2	-3.4 ± 5.0	8.2
16.00	5.8	0.18	3.7	56	4.2 ± 0.4	4.5 ± 0.2	-3.1 ± 4.8	7.9
17.00	6.8	0.18	2.3	61	4.2 ± 0.4	4.5 ± 0.2	-2.1 ± 4.5	7.8
21.83	7.0	0.19	0.72	76	4.2 ± 0.4	3.7 ± 0.2	$+4.2 \pm 4.3$	12.2
23.00	5.4	0.20	0.43	78	3.9 ± 0.4	3.8 ± 0.2	$+1.2 \pm 4.7$	10.5
26.00	7.1	0.21	1.3	83	4.8 ± 0.4	4.0 ± 0.2	$+7.6 \pm 4.6$	15.6